In proceedings of MUCEET2013
Malaysian Technical Universities Conference on Engineering & Technology (MUCET 2013)
December 3–4, 2013, MS Garden Hotel, Kuantan, Pahang, Malaysia
Paper No: UMP–010

Estimation of Heat Transfer and Pressure Drop in an In–Line Flat Tubes Bundle by Radial Basis Function Network (RBFN)

Tahseen Ahmad Tahseen[1,3,*], M. Ishak[1,2,*] and M.M. Rahman[1,2]

[1]Faculty of Mechanical Engineering, University Malaysia Pahang
26600 Pekan, Pahang, Malaysia
Phone: +609–424–2246; Fax: +609–424–2202
[2]Automotive Engineering Centre, Universiti Malaysia Pahang,
26600 Pekan, Pahang, MALAYSIA
[3]Department of Mechanical Engineering, College of Engineering, Tikrit University,
Tikrit, IRAQ
[*]E–mail: tahseen444@gmail.com & tahseen@tu.edu.iq ; mahadzir@ump.edu.my

Abstract

This paper presents how to predict the heat transfer and pressure drop for in–line flat tubes configuration in a crossflow using an artificial neural networks (ANNs). The numerical study of a 2–D steady state and incompressible laminar flow in a tube configuration is also considered in this study. A finite volume technique and body–fitted coordinate system used to solve the Navier–Stokes and energy equations. The Reynolds number based on hydraulic diameter varies from 10 to 320. Heat transfer coefficient and pressure drop results are presented for tube configurations at three transverse pitches are 2.5, 3.0 and 4.5 with two longitudinal pitches are 3.0 and 6.0. The predicted results for average Nusselt number and dimensionless pressure show a good agreement with available previous work. The accuracy between actual values and ANNs approach model results was obtained with a mean relative error less than 4.10% for average Nusselt number and less than 4.8% for pressure drop.

Keyword: In–line flat tube; Finite volume technique; Modeling; Radial basis function network.

1. Introduction

The fluid flow and heat transfer in tube banks symbolize an idealization of many industrial significant processes. Tube bundles are widely employed in cross–flow heat exchangers, the design is still based on empirical correlations of heat transfer and pressure drop. Heat exchangers with tube banks in a cross–flow are of great practical interest in many thermal and chemical engineering processes [1–4]. Flat tube designs have been newly introduced for use in modern heat exchanger applications such as automotive radiators. Flat tube seems to have appropriate pressure drop characteristics compared to circular tubes [5]. The forced convection heat transfer over a bundle of circular cylinder was investigated numerically Jang et al. [6] and non–square tube in–line arrangements, both the in–line and staggered tube arrangement [7]. The flow over elliptic cylinders bank of tubes presented from Yianneskis et al. [8] both numerically and experimentally. Tahseen et al. [9–11] did numerical studies incompressible, on steady state flow and using the body fitted coordinate (BFC). The studies are heat transfer over a two flat tube with staggered configuration. The second study heat transfer over a series of the flat tube between two parallel plates and third study heat transfer over in–line circular tube banks. The all studies show the effect of Reynolds number on the average Nusselt number. The average Nusselt number increases with increases of Reynolds number.
Artificial neural networks have been used in many engineering applications because of providing better and more reasonable solutions [12,13]. A feed–forward back–propagation ANN using by Ermis et al. [14] to analyse the heat transfer of phase change process in an around the finned tube, the study both numerical and experimental. The mean relative error of 5.58% at the experimental while numerical model ends up to 14.99%. Fadare and Fatona [15] have studied ANN in modelling of a staggered multi–row, multi column in cross–flow, tube to tube heat exchanger and the experimental data for air flow over a bundle of tubes. The results show that the mean absolute relative error less than are 4% and 1% for the testing and training data sets, respectively. Islamoglu and Kurt [16] used the ANNs model for predicted the heat transfer in corrugated channel. The error between the experimental results and ANNs approach the approximation of the mean absolute relative error is less than 4%.

Therefore, this study also focused on the applicability of Radial basis function network method for heat transfer analysis and pressure drop over an in–line flat tube banks, utilize in the design of heat exchangers to promote heat transfer.

2. Mathematical Formulation

Four isothermal heated horizontal flat tube in row. The flat tube have two diameters the transverse, d_T and the longitudinal, d_L the surface temperature of tube T_s placed in the velocity U_{in} and the uniform inlet free stream of temperature T_{in} in the in–line arrangement. The longitudinal pitch–to–small diameter ratio $P_L = P_1/d_T$ are 3.0 and 6.0 as well as the transverse pitch–to–small diameter ratio $P_T = P_2/d_T$ are 2.5, 3.5 and 4.5. The flat tube to be long enough so that it can be neglected the end effect of tube. Therefore it can be assumed the flow field to be two–dimensional. The tubes configuration and flow calculated fields for in–line flat tube banks as shown in Figure 1a. The governing equations were transformed into dimensionless forms upon incorporating the following non–dimensional variables.

$$\left.\begin{array}{lll} (X,Y)=\dfrac{(x,y)}{D_h}, & P=\dfrac{p}{\rho\times(U_{in})^2}, & (U,V)=\dfrac{(u,v)}{U_{in}}, \\ \theta=\dfrac{T-T_{in}}{T_s-T_{in}}, & Re=\dfrac{U_{in}\times D_h}{\nu}, & Pr=\dfrac{\mu c_P}{k} \end{array}\right\} \quad (1)$$

where (x,y) are the Cartesian coordinates, m; ρ the air density, kg/m^3; p pressure, N/m^2; U_{in} the inlet velocity of air, m/s; (u,v) the velocity components of fluid, m/s; T fluid temperature, ^oC; T_{in} inlet free stream temperature, ^oC; T_s surface temperature of tube, ^oC; D_h hydraulic diameter of tube, m; μ the air dynamic viscosity, kg/(m s); c_P the air specific heat J/(kg K) and k the air thermal conductivity W/(m K).
In developing the model, the following assumptions were made: (i) the physical properties of air flow are constant; (ii) the air flow is incompressible and laminar flow; and (iii) the steady states flow and heat transfer. The governing equations for two–dimensional continuity, Naviere–Stokes for momentum and energy equation can be written as follows [17].

The continuity equation

$$\nabla.\,\mathrm{v}=0 \quad (2)$$

Momentum (Navier–Stokes) equation

$$\rho\nabla(\mathrm{vv})=-\nabla P+\mu\nabla.(\nabla\mathrm{v}) \quad (3)$$

Energy equation

$$\nabla(\mathrm{vT})=\frac{k}{\rho c_P}\nabla.(\nabla\mathrm{T}) \quad (4)$$

In expression (2) and (3), v is the velocity vector (u,v).
The physical system considered in the present study is displayed in Figure 1a. The boundary conditions used for the solution domain are uniform inlet velocity, fully developed outflow, and a combination of symmetry and no–slip tube surfaces on the bottom and top boundaries. To complete the formulation of the issue, the boundary conditions are determined to simplify the two–dimensional solution domain as is illustrated in Figure 1a. The boundary conditions can summarize as below;
The entrance the domain: $U=1,\ V=\theta=0$
Symmetric lines: $\partial U/\partial Y=0,\ V=0,\ \partial\theta/\partial Y=0$
The exit of the domain: $\partial U/\partial X=0,\ \partial V/\partial X=0, \partial\theta/\partial X=0$
The surface of tubes: $U=0,\ V=0,\ \theta=1$
The set of conservation Equations (2)–(4) can be written in general form in Cartesian coordinates as Equation (5).

$$\frac{\partial(U\phi)}{\partial X}+\frac{\partial(V\phi)}{\partial Y}=\frac{\partial}{\partial X}\left(\Gamma\frac{\partial\phi}{\partial X}\right)+\frac{\partial}{\partial Y}\left(\Gamma\frac{\partial\phi}{\partial Y}\right)+S_\phi \quad (5)$$

The continuity equation, Equation (2) has no diffusion and source terms. It will be used to derive an equation for the pressure correction. The grid generation scheme based on elliptic partial differential equations is used in the present study to generate the curvilinear coordinates. Equation (5) can be transformed from the physical domain to the computational domain according to the following transformation $\xi = \xi(x, y), \eta = \eta(x, y)$ [18,19]. The schematic of computational grid as is illustrated in Figure 1b.
The final form of the transformed equation can be written as Equation (6).

$$\frac{\partial}{\partial \xi}(\phi G_1) + \frac{\partial}{\partial \eta}(\phi G_2) = \frac{\partial}{\partial \xi}\left[\frac{\Gamma}{J}\left(\alpha \frac{\partial \phi}{\partial \xi} + \gamma \frac{\partial \phi}{\partial \eta}\right)\right] + \frac{\partial}{\partial \eta}\left[\frac{\Gamma}{J}\left(\beta \frac{\partial \phi}{\partial \eta} + \gamma \frac{\partial \phi}{\partial \xi}\right)\right] + J \times S_\phi \tag{6}$$

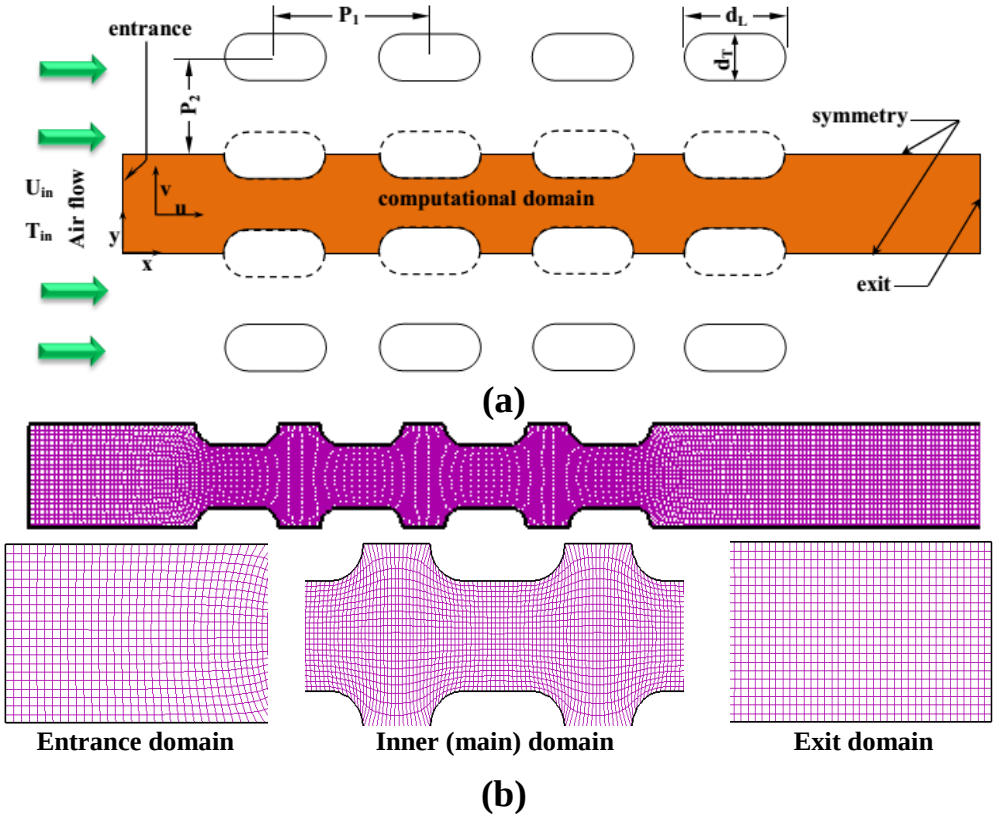

Figure 1: In–line flat tube bank (a) tube arrangement and computational domain, and (b) schematic of computational grid systems generated by the body–fitted coordinates.

They are expressed as

$$\left.\begin{aligned} G_1 &= U\frac{\partial Y}{\partial \eta} - V\frac{\partial X}{\partial \eta}, \qquad G_2 = V\frac{\partial X}{\partial \xi} - U\frac{\partial Y}{\partial \xi}, \\ J &= \frac{\partial X}{\partial \xi}\frac{\partial Y}{\partial \eta} - \frac{\partial Y}{\partial \xi}\frac{\partial X}{\partial \eta}, \qquad \alpha = \left(\frac{\partial x}{\partial \eta}\right)^2 + \left(\frac{\partial y}{\partial \eta}\right)^2, \\ \beta &= \left(\frac{\partial x}{\partial \xi}\right)^2 + \left(\frac{\partial y}{\partial \xi}\right)^2, \quad \gamma = \left(\frac{\partial x}{\partial \xi}\frac{\partial x}{\partial \eta}\right) + \left(\frac{\partial y}{\partial \xi}\frac{\partial y}{\partial \eta}\right) \end{aligned}\right\} \tag{7}$$

In this study the finding of the overall pressure drop and Nusselt number for the resulting air flow and temperature fields are expect the total pressure drop for the flat tube bank system is represented using a dimensionless pressure drop, *CP* and average Nusselt number, $\overline{Nu}$ [20] defined as.

$$\overline{Nu} = \frac{\bar{h} \times D_h}{k}, \quad CP = \frac{2 \times (P_{in} - P_{out})}{\rho \times (U_{in})^2 \times N_L} \tag{8}$$

where N_L is number of tube in deep of row.

2.1. Numerical Methods

The governing equations are solved numerically using FORTRAN 95 (FTN95). The computer code solved the equation of continuity, momentum and energy discretized using a finite–volume technique based on non–orthogonal coordinate system with Cartesian velocity components and non–staggered (collocated) grid [21] with cooperation of the SIMPLE algorithm [22,23]. The has been monitoring the convergence to steady state using determine of iterator–to iterator variations of a field variable normalized by its domain. The normalized maximum root mean square (RMS) defined as

$$\text{RMS} = \frac{|\chi_{new} - \chi_{old}|}{(\chi_{max} - \chi_{min})} \tag{9}$$

where χ were U, V, P, and θ. The value of RMS has been checked in all nodal locations and announced convergence when the upper values of RME were typically less than 1×10^{-4}.
The numerical model was validated with some of previously published standard problems. The comparison between the code results and Bahaidarah et al.[24] it can be seen in previous published [25].

2.2. Calculation procedure for the Generalized Radial Basis Functions Neural Networks

The artificial neural network is an information processing system has certain properties in a joint performance with biological neural networks. As the artificial neural networks are one of the commonly used and developed models to investigate of relationship between linear or non–linear input–output patterns. Moreover, they try to circulate training team and then approximation the test team. Performance is measured using RBFN with predictable success. There are a lot literature give a detailed ANN types related with the function approximation. Schematic diagrams for some artificial intelligence models used in the analysis are shown in Figure 2. The neural networks are using MATLAB programed and all tests have been implemented in a computer. Activate the error function used in this study is a function of the logistic sigmoid and standard total of squared error function, respectively.

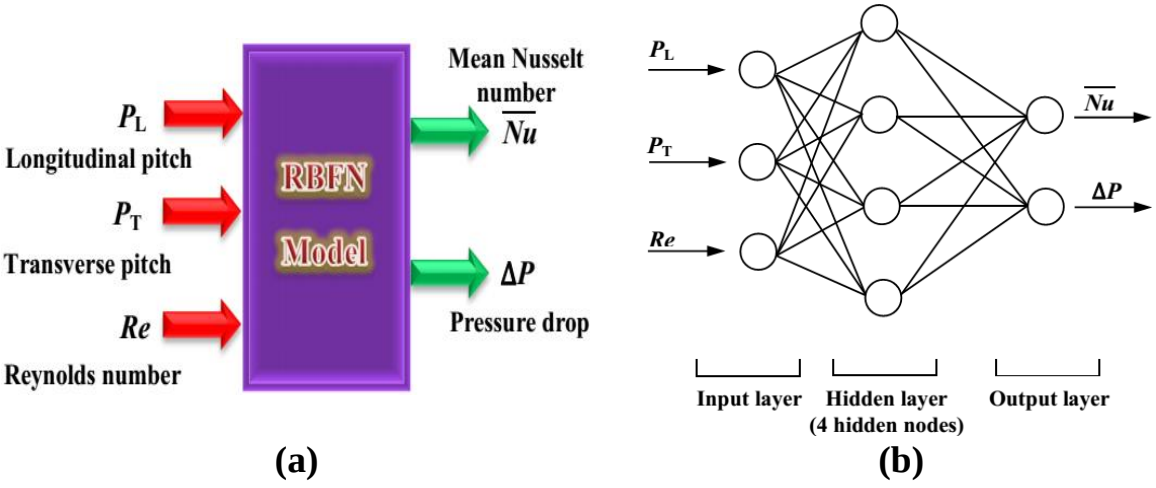

Figure 2: Schematic of system models (a) input and output, and (b) the Radial Basis Functions Neural Networks.

The data was evaluated numerically in this study are normalized in order to get the values. The formula used is the following

$$\frac{\text{Actual value} - \text{Minimum}}{\text{Maximum} - \text{Minimum}} \times (\text{High} - \text{Low}) + \text{Low} \tag{10}$$

Where maximum is the maximum data value, minimum is minimum data value, low is the minimum normalized data value = 0.1, and high is the maximum normalized data value = 0.9 [26].

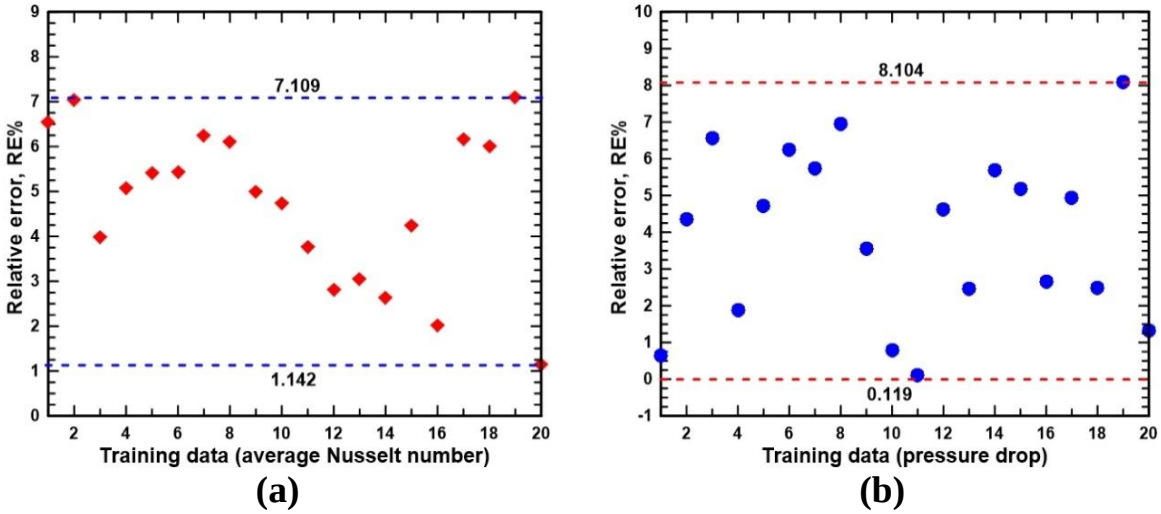

Figure 3: The relative error for training data using (a) average Nusselt number, and (b) pressure drop.

3. Results and Discussion

The numerical performances were conducted to verify the results from the RBFN model. Sixty numerical simulation data were used to construct the model of RBFN. To improve of the model proposed of twenty data (about 2/3×100%) it is used for training and ten data the remainder for testing performance (about 100/3%) were used to test the RBFN model.

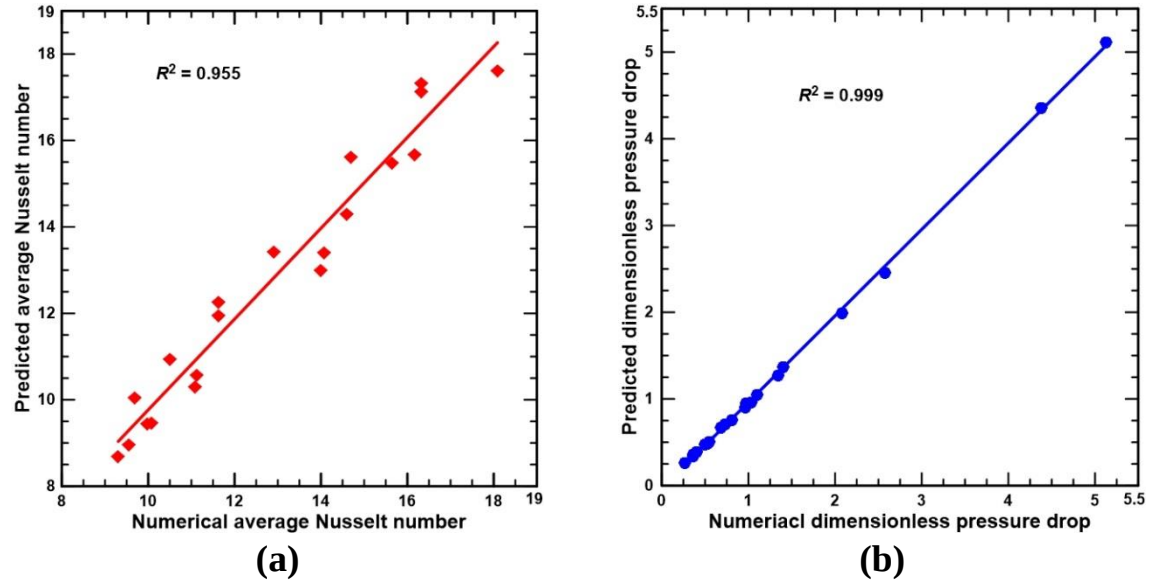

Figure 4: Scatterplots of the training data for (a) average Nusselt number, and (b) dimensionless pressure drop.

The relative error results of RBFN model shown in Figure 3 for training data, where the relative error (RE) for variable *B* and the Mean Relative Error (MRE) are estimated as [27].

$$E\% = \frac{|\psi_{Num} - \psi_{Pre}|}{\psi_{Num}} \times 100, \quad MRE\% = \frac{1}{n}\sum_{i=1}^{n}(RE\%)_i \tag{11}$$

Where (Num), (Pre) and (N) are stand for numerical values, predicted values and the number of numerical data, respectively.

Table 1: Comparison the average Nusselt number and dimensionless pressure drop of numerical and RBFN model for testing data.

Run no.	1	6	7	11	12	16	21	22	26	27
Average Nusselt number										
Numerical	6.51	5.87	8.38	5.62	8.02	6.59	5.94	8.74	5.70	8.38
RBFN	6.32	5.45	7.99	5.89	7.68	6.37	6.30	9.22	6.10	8.01
%RE	3.03	7.04	4.62	5.05	4.24	3.32	5.97	5.48	6.96	4.45
%MRE	5.02									
Dimensionless Pressure drop										
Numerical	17.82	9.41	2.32	6.97	1.71	19.41	10.10	2.67	7.32	1.93
RBFN	16.57	8.88	2.21	6.75	1.58	18.37	9.87	2.61	7.03	1.90
%RE	6.99	5.63	4.54	3.14	7.79	5.39	2.27	2.18	4.04	1.88
%MRE	4.38									

The result of RBFN model for training and testing data shown in Figures 3,4 and 5. From the figures it shows the average Nusselt number and dimensionless pressure drop. It has been observed from Table 1 and Figures 3a, 4a and 5a that for the best ANN arrangement gain in this study, for average Nusselt number the maximum relative error are approximately 7.11% (for training data) and 7.04% (for testing data), and the mean relative error are 4.73% and 5.02%, respectively. As a consequence, the ranges for the relative error values are between 1.14%–7.11% for training and 3.03%–7.04% for testing.

Once, it was spotted from Table 1 and Figures 3b, 4b and 5b that for the best ANN arrangement gain for dimensionless pressure drop the maximum relative error are approximately 8.10% (for training data) and 7.79 % (for testing data). The mean relative errors are 3.96% and 4.38% for training and testing data, respectively. Eventually, the ranges of relative error values are between 0.12%–8.14% training and 1.89%–7.79% for testing.

4. Conclusions

This article the model developed using RBFN to estimate the heat transfer coefficient and pressure drop in a crossflow over an in–line flat tubes bank. The following conclusions were obtained:

(i) For the average Nusselt number, the maximum relative error for trained is 7.2% and the mean relative error is 4.73%. Also, for the testing data is 7.04% and 5.02%, respectively.

(ii) For the dimensionless pressure drop, the maximum relative error for trained is 8.10% and the mean relative error is 3.96%. Also, for the testing data is 7.79% and 4.38%, respectively.

(iii) The prediction of the average heat transfer coefficient and pressure drop with the RBFN models is in good agreement with the numerical result, and also has a smaller error.

(iv) Finally, this study clearly shows that the RBFN model is better for predicting the heat transfer rate and pressure drop in an in–line flat tube bank with comprehensive performance.

Acknowledgements

The authors would like to acknowledgements the Universiti Malaysia Pahang for sponsoring the presented work under the Grant no. GRS130310.

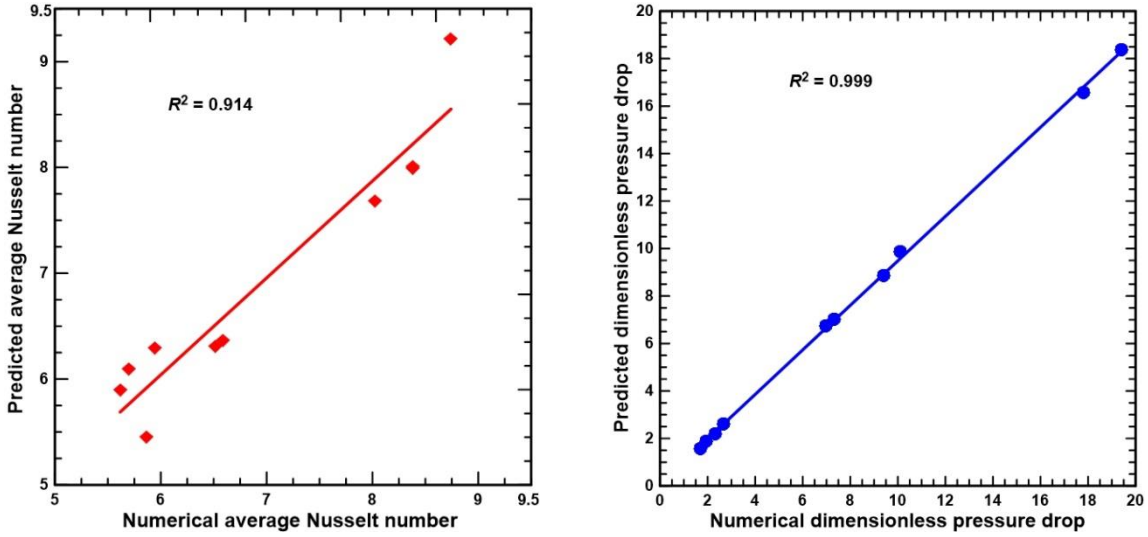

Figure 5: Scatterplots of the testing data for (a) average Nusselt number, and (b) dimensionless pressure drop.

References

[1] Žukauskas, A., 1972, "Heat Transfer from Tubes in Crossflow," Advances in Heat Transfer 8, 93–158.

[2] Benarji, N., Balaji, C. and Venkateshan, S.P., 2007, "Unsteady Fluid Flow and Heat Transfer Over a Bank of Flat Tubes," Heat and Mass Transfer, 44(4): 445–461.

[3] Kaptan, Y., Buyruk, E. and Ecder, A., 2008, "Numerical Investigation of Fouling on Cross–Flow Heat Exchanger Tubes with Conjugated Heat Transfer Approach," International Communications in Heat and Mass Transfer, 35(9): 1153–1158.

[4] Bergman, T.L., Lavine, A.S., Incropera, F.P. and Dewitt, D.P., 2011, "Fundamentals of Heat and Mass Transfer," 7th Edition. New York, USA: John Wiley & Sons Inc.

[5] Webb, R.L. and Kim, N.–H., 2005, Principl of Enhanced Heat Transfer. 2nd Edition. New York, USA: Taylor & Francis Group.

[6] Jang, J.–Y., Wu, M.–C. and Chang, W.–J., 1996, "Numerical and Experimental Studies of Three Dimensional Plate–Fin and Tube Heat Exchangers," International Journal of Heat and Mass Transfer, 39(14): 3057–3066.

[7] Wung, T.–S., & Chen, C.J., 1989, "Finite Analytic Solution of Convective Heat Transfer for Tube Arrays in Crossflow: Part 1– Flow Field Analysis," Journal of Heat Transfer, 111(3): 633–640.

[8] Yianneskis, M., Papadakis, G., Balabani, S. and Castiglia, D., 2011, "An Experimental and Numerical Study of the Flow Past Elliptic Cylinder Arrays," Proceedings of the Institution of Mechanical Engineers, part C: Journal of Mechanical Engineering Science, 215(11): 1287–1301.

[9] Tahseen, T.A., Ishak, M. and Rahman, M.M., 2012, "Analysis of Laminar Forced Convection of Air for Crossflow Over Two Staggered Flat Tubes," International Journal of Automotive and Mechanical Engineering (IJAME), 6: 753–765.

[10] Tahseen, T.A., Ishak, M. and Rahman, M.M., 2012, "A Numerical Study of Forced Convection Heat Transfer Over a Series of Flat Tubes between Parallel Plates," Journal of Mechanical Engineering and Sciences (JMES), 3: 271–280.

[11] Tahseen, T.A., Ishak, M. and Rahman, M.M., 2013, "A numerical Study Laminar Forced Convection of Air for In–Line Bundle of Cylinders Crossflow," Asian Journal of Scientific Research, 6(2): 217–226.

[12] Lin, T.Y. and Tseng, C.H., 2000, "Optimum Design for Artificial Neural Networks: An Example in a Bicycle Derailleur System," Engineering Applications of Artificial Intelligence, 13(1): 3–14.

[13] Genel, K., Ozbek, I., Kurt, A. and Bindal, C., 2002, "Boriding Response of Aisi W1 Steel and use of Artificial Neural Network for Prediction of Borided Layer Properties," Surface and Coatings Technology, 160(1): 38–43.

[14] Ermis, K., Erek, A. and Dincer, I., 2007, "Heat Transfer Analysis of Phase Change Process In a Finned–Tube Thermal Energy Storage System using Artificial Neural Network," International Journal of Heat and Mass Transfer, 50(15–16): 3163–3175.

[15] Fadare, D.A. and Fatona, A.S., 2008, "Artificial Neural Network Modeling of Heat Transfer in a Staggered Cross–Flow Tube–Type Heat Exchanger," The Pacific Journal of Science and Technology, 9(2): 317–323.

[16] Islamoglu, Y. and Kurt, A., 2004, "Heat Transfer Analysis using ANNs with Experimental Data for Air Flowing in Corrugated Channels," International Journal of Heat and Mass Transfer, 47(6–7): 1361–1365.
[17] Bejan, A., 2004, Convection Heat Transfer. 2nd Edition. USA: John Wiley & Sons Inc.
[18] Tannehill, J.C., Anderson, D.A. and Pletcher, R.H., 1997, Computational Fluid Mechanics and Heat Transfer. 2nd Edition. USA: Taylor & Francis.
[19] Thompson, J.R., Warsi, Z.U.A. and Martin, C.W., 1997, Numerical Grid Generation, Foundations and Applications, USA: North–Holland.
[20] El–Shaboury, A.M.F. and Ormiston, S.J., 2005, "Analysis of Laminar Forced Convection of Air Crossflow in In–Line Tube Banks with Nonsquare Arrangements," Numerical Heat Transfer, part A, 48(2): 99–126.
[21] Ferziger, J.H. and Perić, M., 1999, Computational Methods for Fluid Dynamics, 3rd Edition. USA: Springer–Verlag Berlin Heidelberg.
[22] Patankar, S.V., 1980, Numerical heat transfer and fluid flow, USA: Hemisphere, Washington, DC.
[23] Versteeg, H.K. and Malalasekera, W., 2007, An Introduction to Computational Fluid Dynamics: the Finite Volume Method, 2nd Edition. UK: Prentice Hall.
[24] Bahaidarah, H.M.S., Anand, N.K. and Chen, H.C., 2005, "A Numerical Study of Fluid Flow and Heat Transfer Over a Bank of Flat Tubes," Numerical Heat Transfer, Part A, 48(4): 359–385.
[25] Tahseen, T. A., Ishak, M. and Rahman, M. M., 2013, "Performance Predictions of Laminar Heat Transfer and Pressure Drop in an In–Line Flat Tube Bundle Using an Adaptive Neuro-Fuzzy Inference System (ANFIS) Model," International Communications in Heat and Mass Transfer, (in press).
[26] Nasr, G.E., Badr, E.A. and Joun, C., 2003, "Backpropagation Neural Networks for Modeling Gasoline Consumption," Energy Conversion and Management, 44(6): 893–905.
[27] Hayati, M., Rezaei, A. and Seifi, M., 2009, "Prediction of the Heat Transfer Rate of a Single Layer Wire–on–Tube Type Heat Exchanger using ANFIS," International Journal of Refrigeration, 32(8): 1914–1917.

Nomenclature

c_P	specific heat capacity of fluid, J/(kg K)	u, v	velocity components, m/s
CP	dimensionless pressure drop	U, V	dimensionless velocity
d_L	longitudinal diameter of tube, m	x, y	Cartesian coordinates, m
d_T	transverse diameter of tube, m	X, Y	dimensionless Cartesian coordinates
D_h	hydraulic diameter of tube, m	***Greek symbols***	
G_1, G_2	contravariant velocity components	α, β, γ	coefficients of transformation
$\bar{h}$	average heat transfer coefficient, W/(m^2 K)	μ	dynamic viscosity, kg/(m s)
J	Jacobian of the transformation	υ	kinematic viscosity, m^2/s
k	thermal conductivity of fluid, W/(m K)	ρ	density, kg/m^3
N_L	number of tubes in deep row	ξ, η	curvilinear coordinates
$\overline{Nu}$	average Nusselt number	ϕ	general dependent variable
p	pressure, Pa	θ	dimensionless temperature
P_1	longitudinal distance, m	Γ	diffusion coefficient
P_2	transverse distance, m	***Subscripts***	
P_T	transverse pitch	*in*	*in*
Re	Reynolds number	L	longitudinal
S	source term	*out*	*out*
T	temperature, ^{o}C	T	transverse